

Periodic Tip Splitting Instability

B. Utter, R. Ragnarsson and E. Bodenschatz

Laboratory of Atomic and Solid State Physics, Cornell University, Ithaca, NY 14853

(September 14, 1999)

We report experimental results on the tip splitting instability in diffusion limited growth in a directionally solidified succinonitrile-poly(ethylene oxide) alloy. The grain is oriented in the $\{111\}$ plane so the surface tension is nearly isotropic leading to seaweed or dense branching morphology. When following a single dendrite over long times, a periodic tip splitting mechanism is observed in which the tip regularly alternates between splitting towards the left side of the dendrite and splitting to the right. The tipsplitting frequency is found to be related to the growth velocity as a power law with an exponent of 1.66. We also measure the fractal dimension of the interface as a function of growth velocity and find tentative agreement with previous results.

PACS number(s): 68.70.+w, 81.30.Fb

Directional solidification of binary alloys has received considerable attention over the last fifty years as a good example of a non-equilibrium pattern forming system with technological importance. More recently, there has been a growing awareness of the role that surface tension anisotropy plays in selecting the steady state operating condition of the dendrite, known as the solvability condition [1]. Numerous studies have been performed on the typical growth forms of crystals with low, but non-zero, anisotropy, such as cells and dendrites. However, the effective anisotropy depends not only on the crystal itself, but also on the orientation of the crystal with respect to the growth direction. When grown in the $\{111\}$ plane, the surface tension is nearly isotropic and the growth is irregular and constantly tip splitting [2]. This has been called seaweed growth [3], or dense branching morphology [4], and has been observed in such different systems as viscous fingering [5], bacterial colonies [6], electrodeposition [7], annealing of magnetic films [8], and drying water films [9]. Very little work has been done on solidification systems with isotropic effective surface tension, particularly on the dynamics and temporal behavior.

In this Letter, we report experimental results on directional solidification of succinonitrile-poly(ethylene oxide) oriented in the $\{111\}$ plane which exhibit a periodic splitting instability. The tip splitting frequency versus growth velocity shows a power law dependence. To our knowledge, neither the scaling nor the regularly alternating splitting have been predicted theoretically. We also measure the fractal dimension and compare the results to previous predictions and measurements for seaweed growth.

The surface tension anisotropy is based on the underlying cubic structure of the growing solid. Under typical conditions in low speed directional solidification, the orientation of the dendrites and sidebranches is determined by the crystalline structure and the imposed temperature gradient. Changing the angle between the crystalline axis and the pulling direction changes the degree and orienta-

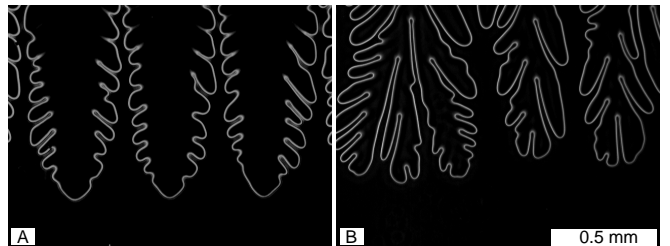


FIG. 1. (A) A dendrite and (B) seaweed structure which differ only in crystalline orientation. The white line indicates the solid-liquid interface. The solid grows downwards into the undercooled melt. The thermal gradient (18 K/cm), concentration (0.25% PEO), and growth velocity ($2.71 \mu\text{m/s}$) are identical in both pictures.

tion of the effective anisotropy [2, 10] which reveals itself as a tilt in the growth direction. Because of the cubic symmetry, growth in the $\{111\}$ plane has an effective surface tension that is close to isotropic.

Without anisotropy of surface tension, the growth lacks the apparent orientation or tilt observed in traditional directional morphologies. As shown in Figure 1B, under the same growth conditions, seaweed structures are very disordered compared to more familiar arrays of cells and dendrites (1A). There does appear to be a typical spacing between the large seaweed lobes, but these are unstable and continuously change over time. The constant tip splitting and competition between lobes leads to the characteristic meandering of the seaweed. This is quite familiar in viscous fingering in particular, which has been a well studied, isotropic system [5].

Brener et al. propose a morphology diagram involving the degree of anisotropy and the undercooling [11]. In this diagram, they distinguish between seaweed structures at low anisotropy and dendritic structures at high anisotropy and between fractal growth at low undercooling and compact growth at large undercooling. They theorize that the fractal structure forms because tip splitting occurs randomly when the strength of the thermal noise is large enough to destabilize the tip [11-12].

At higher anisotropies, the noise is no longer able to destabilize the tip, but might still be important in inducing sidebranching. Efforts have been made to determine whether the sidebranches are created by selective noise amplification or whether they are a global mode of the system, with a noise-independent frequency [13-16]. We believe that dynamic studies of the seaweed morphology might offer more information about the role of noise in solidification.

Others have observed the seaweed morphology in directional solidification. In particular, Akamatsu and Faivre have performed directional solidification experiments studying the effect of surface tension anisotropy and grain orientation on morphology [2, 10]. Ihle and Müller-Krumbhaar have used numerical simulations to study seaweed morphology and its fractal dimension [3]. However, no specific study has been made concerning the temporal behavior or the dynamics of the tipsplitting events.

The present experiment is performed with a traditional directional solidification apparatus in which a thin sample ($13\text{ cm} \times 1.5\text{ cm} \times 50\text{ }\mu\text{m}$) is pulled through a linear temperature gradient at a constant pulling velocity. The cell is pulled by a linear stepping motor with 4 nm step size. In these experiments, the gradient is maintained at about 18 K/cm with a stability of $\pm 5\text{ mK}$ on each side. The sample is a 0.25% poly(ethylene oxide) [17] in succinonitrile alloy, which has a low partition coefficient ($k \approx 0.01$) and low diffusivity ($D \approx 8 \times 10^{-11}\text{ m}^2/\text{s}$).

The liquid-solid interface is observed with phase contrast microscopy and sequences of images are recorded using a CCD camera with a framegrabber or time lapse video. The interface can then be easily extracted to measure quantities such as curvature and fractal dimension.

To observe the seaweed growth, the sample is melted completely and quenched, seeding numerous grains. One grain with the optimal orientation is selected and all the others are melted off with an argon laser beam. The chosen grain is then allowed to grow and fill the width of the cell. It is important to have a single grain in the cell, since dendrites typically overtake seaweeds during solidification [2].

Space-time plots show the weedy nature and allow us to see where the tip splitting events occur (Fig. 2). These are created by taking the pixels from the 25th row from the top from each image and stacking them sequentially in time. The plot displays the history of the seaweed and is essentially a chart recording of the growth in the absence of further coarsening.

The space-time plot in Figure 2 illustrates two different kinds of splitting events. In one (A), the tip splits but one main branch continues to grow. In the other (B), the tip splits into two or three new branches. These branches compete and strongly interact with each other until either one falls behind or they spread apart far enough so each continues growing as a main branch. Often, if two branches grow, another neighboring lobe will fall behind

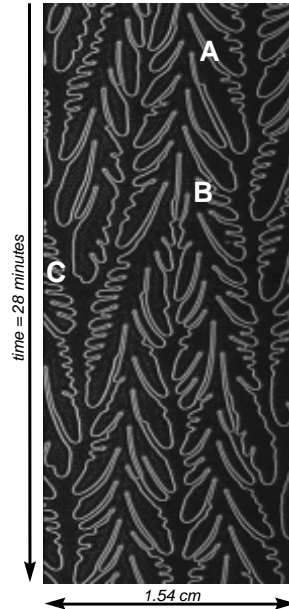


FIG. 2. Space-time plot. Time increases downwards. The total time shown is 28 minutes from a run that lasted approximately 5 hours. The width is 1.54 cm and the growth velocity is $2.71\text{ }\mu\text{m/s}$. The growth exhibits (A) periodic splitting on the right and left sides of the tip, (B) tip splitting in center creating additional main branches, and (C) a branch falling behind as it is crowded from the right.

(C), maintaining a roughly constant number of branches across the cell. These two events (A and B) happen because the indentations that lead to tip splittings can occur at any point on the tip. When a tip splits off-center, the smaller finger typically falls behind much as sidebranches are convected away.

Not only are lobes often being created or falling behind, but the splitting events which occur at different places on the tip create arms of varying lengths, causing the growth to appear random.

It has long been known from free growth that a growing seed will become unstable to perturbations at some specific radius [18]. Therefore, as the seaweed is dominated by tip splitting, it is important to measure curvatures around the tip.

Taking the tip to be the furthest point along the growth direction on a particular lobe, we can extract a segment of the interface around the tip. Then, we measure the curvature of the interface at each point along this arc. The segment used is typically $300\text{ }\mu\text{m}$ long as compared to the tip radii of $25\text{-}75\text{ }\mu\text{m}$. Plotting the curvature versus the position along the arc and combining the plots from different times, we can create curvature-time plots similar to the space-time plots above (Fig. 3). In these curvature-time plots, the greyscale intensity corresponds to the absolute value of the curvature. Note also that the selected arc segment is centered around the tip.

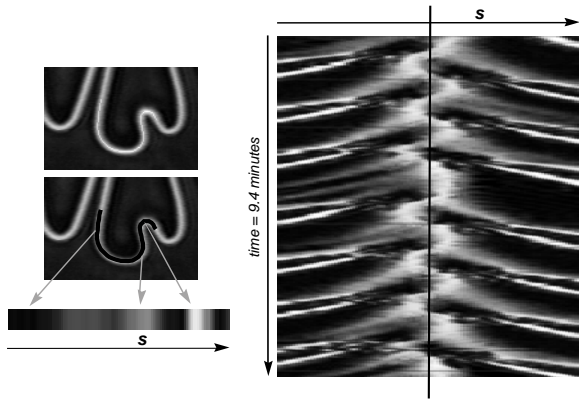


FIG. 3. Curvature-time plot. A representation of the curvatures along the interface near the tip. To the left is a tip region with an segment indicated in black. Below it, the absolute curvatures along this segment are plotted in greyscale. Stacking sequences of these lines in time gives the curvature-time plot on the right, where the center line always corresponds to the tip. The total time shown is 9.4 minutes and increases downwards. The width is approximately $300 \mu\text{m}$ and the growth velocity is $2.71 \mu\text{m/s}$. White corresponds to high curvatures (radius of curvature less than $10 \mu\text{m}$) and black to zero curvature.

The middle third of the curvature profile then shows the curvature in the immediate vicinity of the tip. The bright pairs of lines to the sides represent the very high curvature at a deep groove that is formed when a tip splits and the groove is convected down the sides. The striking feature is that the curvatures at the tip which lead to tipsplittings oscillate (as in A on Fig. 2). This is not simply an artifact of the tip position moving from side to side as the position of the tip changes by a relatively small amount. The tip can be clearly seen to flatten on one side and split while at the same time beginning to flatten on the other side. This is also quite periodic, which calls into question the role of noise at the tip and may indicate a self-sustaining global mode.

The periodicity is broken occasionally (typically after around 10-20 cycles) when the tip splits nearly in the center, forming two main branches (Fig. 2B). These two “new” lobes clearly influence each other by suppressing the tipsplitting on their adjacent sides, reminiscent of double growth in which two symmetry broken dendrites tend to stabilize each other. This may not be so surprising, as doublons are the basis of the compact seaweed expected at high undercoolings [12]. Once one branch falls behind or they are separated enough, the remaining tip continues to oscillate in the way described before. At higher growth velocities, we do find the expected double growth structures, but they are intermittent and short-lived in this grain. As a doublon forms, one of the two arms falls behind and soon thereafter, the remaining arm splits to form another transient doublon.

At each velocity, the tip splitting frequency is mea-

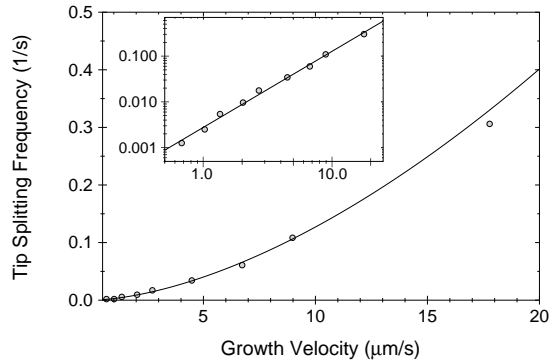


FIG. 4. Tip splitting frequency versus growth velocity. The inset shows the same data on a log-log plot. The fitted line relating the frequency to the velocity is $f = 2.78 \times 10^{-3} * V^{1.66}$.

sured by following one branch over long times. The log-log plot (Fig. 4) of the tip splitting frequency versus growth velocity shows a power law with an exponent of 1.66. This compares to the exponent of 1.5 for side-branching frequency in dendrites [14, 20].

In this range of growth velocities, there is no significant deviation from the power law fit, however, at low speeds, the slight anisotropy in the sample is revealed and splitting events to one side dominated the splits to the other. At high speeds, the structures become smaller and growth is more three dimensional, making it difficult to extract the interface and follow the tip.

Since we expect to see a crossover from fractal to compact structures with increased pulling speeds [11], we measured the fractal dimension of our images by using a standard box counting method (Fig. 5) [19]. The lower physical cutoff of the fractal range is close to the wavelength of the initial instability of the flat interface. The experimental measurement of this value has been indicated on the plot (Fig. 5A).

Figure 5B shows the fractal dimension versus the pulling speed. The circles correspond to fitting over one decade from the initial instability wavelength. The triangles correspond to fitting over 0.43 decades, equivalent to one division on a natural log plot, which has been used in some previous results [3]. It’s clear that the fractal dimension is somewhat sensitive to the range of data taken for the fit, although the general trend seems to remain that the fractal dimension increases with pulling speed. This increase from close to the diffusion limited aggregation value of 1.67 towards 2 would be consistent with Brener et al.’s prediction of a noisy transition from fractal to compact growth, but it doesn’t confirm the predicted discontinuous nature of the transition. In particular, the fit over one decade suggests a discontinuous jump while the smaller fitting region shows a relatively smooth rise.

At first, Figure 5B still looks promising in indicating a transition from fractal to compact growth, but a few issues must be noted. As mentioned, the slope is relatively sensitive to the range of the fit and, at most,

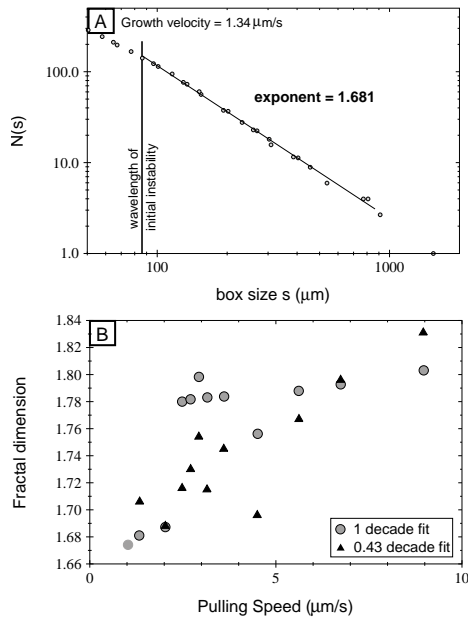


FIG. 5. Fractal analysis. A box counting method is used in which a grid of spacing s is superimposed on a picture of a dendrite and the number of boxes containing any part of the interface ($N(s)$) is counted. (A) A linear region on a log-log plot indicates a fractal range with the dimension given by the slope. The plot here is for a growth velocity of $1.34 \mu\text{m/s}$ and the experimental initial instability wavelength is included as the lower length scale cutoff for the fractal range. (B) Averaging results from 1000 pictures for each point, the fractal dimension versus the pulling speed is plotted.

one decade in length scales can be used. Also, at lower speeds, as the weed tends towards less developed cellular growth, the calculated dimension actually drops towards one rather than levelling out. In other words, these pictures do not exhibit growth that is clearly fractal over a significant range of length scales. The fractal dimension also appears to be most well defined at the tip, as the dimension increases towards 2 when more of the deep groove region is included in the analysis.

These results compare to recent numerical simulations of free growth by Ihle and Müller-Krumbhaar who find a fractal dimension of 1.70 ± 0.03 [3]. Their scaling range is equivalent to the smaller fitting region above and simulations are performed at zero anisotropy which we are not able to obtain experimentally.

In conclusion, experimental studies of the seaweed growth morphology show a surprisingly regular periodicity in tip splitting with a frequency that is related to the growth velocity by a power law with an exponent of 1.66. It remains to be seen whether gradually increasing the anisotropy of the system (as in simulations) would bring the growth back to a dendritic mode with the corresponding exponent for sidebranch frequency of 1.5. Despite the generally disordered patterns of seaweed growth, this periodic splitting at the tip may reveal the possibility a new

mode intrinsic to the system. Also, the apparent disorder of the system is induced by competition between different branches and splitting at different locations on the tip. The fractal dimension is measured and a transition is observed from fractal towards compact. However, it is not clear that the growth exhibits a good fractal scaling over a sufficient span of length scales.

This work made use of the Cornell Center for Materials Research facilities supported by NSF Funded Award #DMR-9632275.

-
- [1] J. S. Langer, in *Chance and Matter*, edited by J. Souletie, J. Vannimenus, and R. Stora (Elsevier, New York, 1987).
 - [2] S. Akamatsu, G. Faivre, and T. Ihle, *Phys. Rev. E*, **51**, 4751 (1995).
 - [3] T. Ihle and H. Müller-Krumbhaar, *Phys. Rev. Lett.*, **70**, 3083 (1993), *Phys. Rev. E*, **49**, 2972 (1994).
 - [4] E. Ben-Jacob, G. Deutscher, P. Garik, Nigel D. Goldenfeld, and Y. Lareah, *Phys. Rev. Lett.*, **57**, 1903 (1986).
 - [5] K. V. McCloud and J. V. Maher, *Physics Reports*, **260**, 139 (1995).
 - [6] T. Matsuyama and M. Matsushita, *Crit. Rev. Microbiol.*, **19**, 117 (1993).
 - [7] O. Zik and E. Moses, *Phys. Rev. E*, **53**, 1760 (1996).
 - [8] C. H. Shang, *Phys. Rev. B*, **53**, 13759 (1996).
 - [9] N. Samid-Merzel, S. G. Lipson, and D. S. Tannhauser, *Physica A*, **257**, 413 (1998).
 - [10] S. Akamatsu and G. Faivre, *Phys. Rev. E*, **58**, 3302 (1998).
 - [11] E. Brener, H. Müller-Krumbhaar, and D. Temkin, *Phys. Rev. E*, **54**, 2714 (1996), E. Brener, H. Müller-Krumbhaar, D. Temkin, and T. Abel, *Physica A*, **249**, 73 (1998).
 - [12] E. Brener, T. Ihle, H. Müller-Krumbhaar, Y. Saito, and K. Shiraishi, *Physica A*, **204**, 96 (1994).
 - [13] U. Bisang and J. H. Bilgram, *Phys. Rev. Lett.*, **75**, 3899 (1995).
 - [14] M. Georgelin and A. Pocheau, *Phys. Rev. E*, **57**, 3189 (1998).
 - [15] A. Karma and P. Pelcé, *Phys. Rev. A*, **39**, 4162 (1989).
 - [16] A. Couairon and J. M. Chomaz, *Phys. Rev. Lett.*, **77**, 4015 (1996).
 - [17] Poly(ethylene oxide) with an attached rhodamine dye (Sulferhodamine Bis-(PEG 2000)), with a molecular weight of 4500, is purchased from Molecular Probes, Inc. (Eugene, OR).
 - [18] W. W. Mullins and R. F. Sekerka, *J. Appl. Phys.*, **34**, 323 (1963).
 - [19] See for instance, H. Peitgen, H. Jürgens, and D. Saupe, *Chaos and Fractals*, (Springer-Verlag, New York, 1992).
 - [20] B. Billia and R. Trivedi, in *Handbook of Crystal Growth*, ed. by D. T. J. Hurle (North-Holland, New York, 1993).